Molecular Crystals and Liquid Crystals
Publication details, including instructions for authors and subscription information:
http://www.tandfonline.com/loi/gmcl16

Electron Spin Resonance of Highly Anisotroic Organic Systems

G. Weill [a] , J. J. Andre [a] & A. Bieber [a]
[a] Centre de Recherches sur les Macromolécules, C.N.R.S., 67083, Strasbourg Cedex, France
Version of record first published: 19 Oct 2010.

To cite this article: G. Weill , J. J. Andre & A. Bieber (1978): Electron Spin Resonance of Highly Anisotroic Organic Systems, Molecular Crystals and Liquid Crystals, 44:3-4, 237-265

To link to this article: http://dx.doi.org/10.1080/00268947808084983

Mol. Cryst. Liq. Cryst., 1978, Vol. 44, pp. 237–266

Printed in Holland

Electron Spin Resonance of Highly Anisotropic Organic Systems†

G. WEILL, J. J. ANDRE and A. BIEBER

Centre de Recherches sur les Macromolécules, C.N.R.S., 67083 Strasbourg Cedex, France

(*Received July 29, 1977*)

After a brief discussion concerning the chemical nature and structural organization, ESR results obtained on low and highly conducting quasi one-dimensional organic systems, are presented. Related to the knowledge of the molecular properties, invaluable informations about the properties of the linear chains may be obtained on single crystals from the susceptibility, the g tensor and the line shape: existence of magnetically inequivalent sites, respective contributions of the different magnetic species (for low conducting systems) or of the different chains (for highly conducting systems). In particular cases, the existence of weak intrachain coupling has been pointed out and even some order of magnitude for the ratio of intra- to interchain exchange have been reached.

1 INTRODUCTION

Theories dealing with one-dimensional systems present many interesting features and there is a large interest for real systems which could exhibit some of these peculiar properties and help to understand the limits of the one-dimensional behaviour due to weak coupling in the other directions.[1–7] Among these real systems, we shall focus our interest on organic "molecular-ionic" crystals.[8,9]

In these large aromatic systems, the magnetic properties of the crystals are likely to retain some of the characteristics of the ESR of isolated-radical ions. We therefore just recall that the ESR signal depends upon the g factor tensor due to residual spin orbit coupling, the hyperfine tensor A which couples the electronic and nuclear spins and the spin relaxation which governs the line shape and line width of individual transitions between different sublevels according to the selection rules $\Delta m = \pm 1$.

† This paper is based on a lecture given at the Conference on Organic Solids, Schloss-Elmau, 1976.

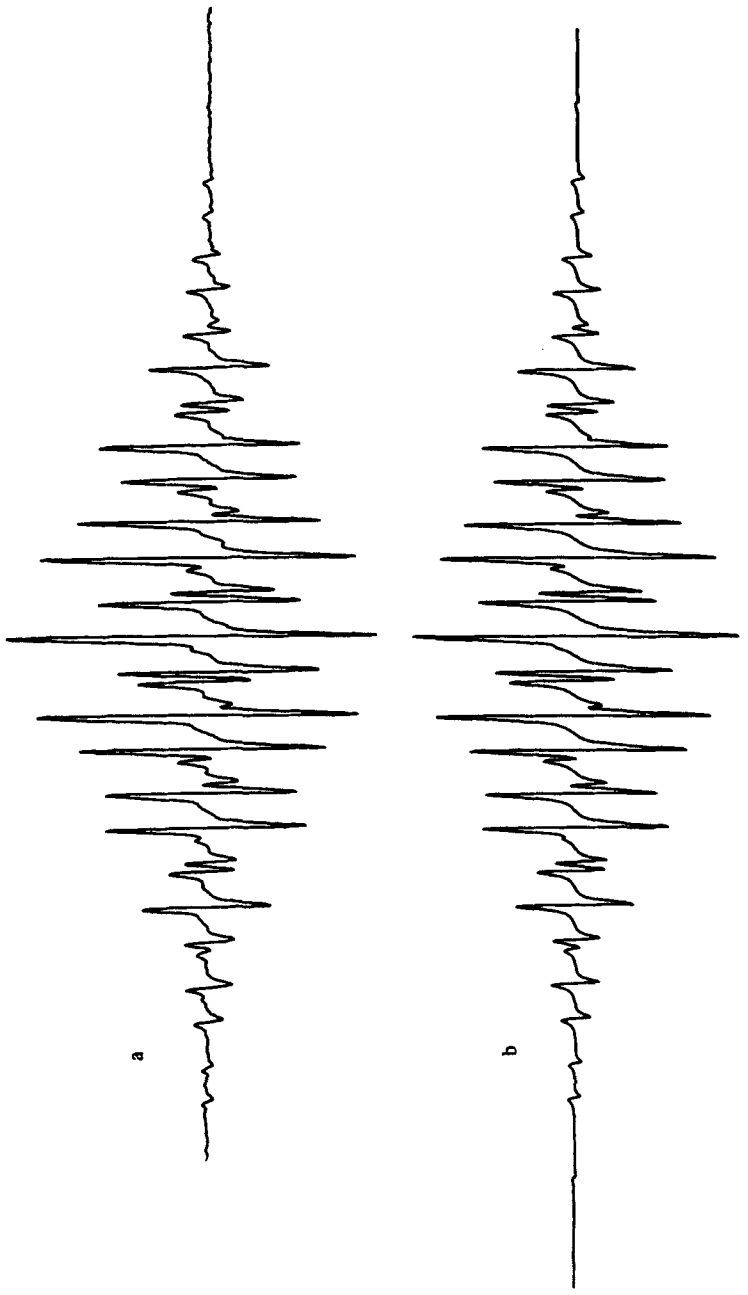

FIGURE 1 ESR spectrum of the radical anion of TCNQ: a) Experimental spectrum obtained from Cu^{+}-$TCNQ^{-}$ in an acetonitrile solution at room temperature: $a_H = 1.416 \pm 0.003$ G, $a_N = 0.987 \pm 0.003$ G; b) Calculated spectrum with Lorentzian line shape (width 0.068 gauss and modulation broadening 0.010 gauss)(unpublished result)

Observation of rapidly tumbling molecules in solution allows only to obtain informations upon the mean g value and the isotropic part of A (Figure 1). Work on *isolated oriented radicals* (as for example the radicals formed by irradiation of crystals) would be necessary for a full determination of the g and A tensors. However work on *dilute frozen solutions* leads, in favourable cases, to the same type of information (Figure 2).

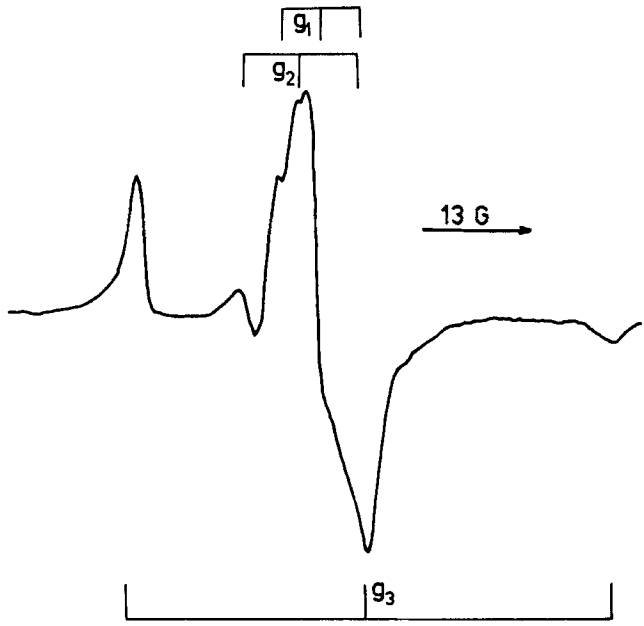

FIGURE 2 Detailed ESR spectrum of 5×10^{-3} M Fremy's salt and 0.5 M KNO_3 in ice at 77 K (taken from Ref. 11).

In more *concentrated* systems, interaction between *localized moments* will manifest in dipolar and exchange interactions. The first one tends to broaden the spectrum whereas the second one modulates the dipolar and hyperfine interactions and leads to a sharpening of the line.[13]

Molecular ionic crystals, which we are dealing with in this paper, form a particular class of molecular crystals involving cyclic planar molecules where π electrons play a dominant role. Our aim is to stress how ESR techniques can contribute to the qualitative and quantitative understanding of these systems. This is done in Sections 3 and 4 after a brief summary of some of their properties given in Section 2.

2 LINEAR ORGANIC SYSTEMS

In these systems, the electronic properties, in particular the electrical conductivity, may be unusual for organic compounds. The values of the electrical conductivity, at room temperature, are distributed over a large range. In general the temperature dependence of the conductivity is very different between systems. We shall distinguish the highly conducting systems and the low conducting systems.[7]

Crystals of large π aromatic systems cannot be considered as simple collections of paramagnetic molecules; due to the large orbital overlap, charge transfer interaction plays a major role in the charge distribution on the different molecules in a stack.[7]

Let us give a picture, from both a chemical and a structural point of view, of the systems which have been recognized and studied as quasi one-dimensional ones. These systems have been classified according to at least two criteria: chemical nature and structural organization. We can distinguish:[7]

a) Chemically:	1. Free radicals	A. Stoichiometry 1 : 1
	2. Radical ions-salts (RIS)	B. Stoichiometry $n : m$
	3. Charge transfer complexes (CTC)	$(n \neq m)$
b) Structurally:	1. Segregated chains	A. Regular
	2. Mixed chains	B. Alternated

which can combine to give a number of classes. The most important ones are schematically represented in Table I.

It must however be realized that in real structures the molecular planes are generally not perpendicular to the chain axis and that the overlap is strongly dependent upon the relative lateral displacements of the molecules (Figure 5). Hence the "alternation," as deduced from a doubling of the unit cell, does not imply a large difference in *distances* between the molecular planes. A high resolution in the crystallography of such compounds is needed either to integrate the total electronic density or to detect deformations of the molecular plane and changes in intramolecular distances. Both methods have been used to get informations about the charge distribution.[7]

From a detailed examination of the chemical and crystalline structures, it appears that all highly conducting systems are either RIS or ionic CTC (i.e. with a large charge transfer amount) with segregated RI chains, regular stackings, very short inter-molecular distances, large electronic overlaps and polarizable cations.

No complete unambiguous interpretation of the physical properties is yet available either for highly conducting or low conducting systems. For the low conducting systems no general model has yet been suggested in contrast to

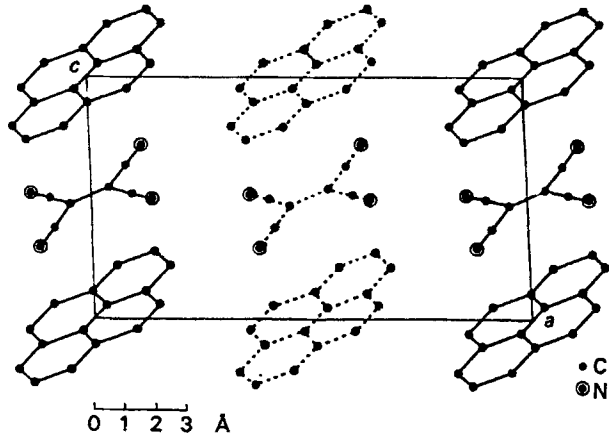

FIGURE 3 Crystalline structure of 1 : 1 CTC Pyrene-TCNE (projection 010). Stacks are parallel to c axis (reproduced with permission of Ref. 14).

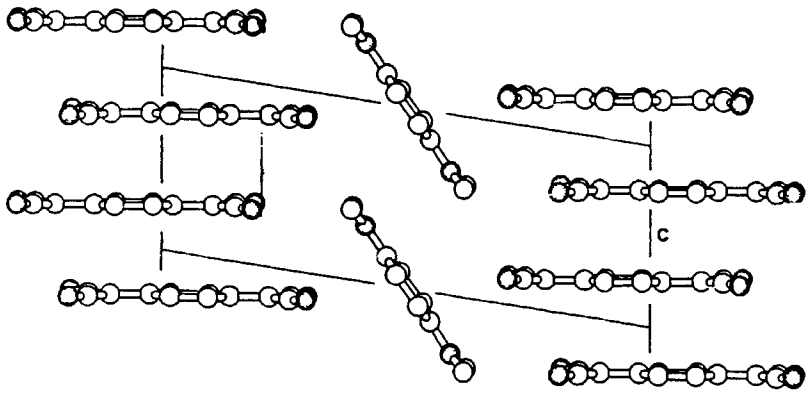

FIGURE 4 Crystalline structure of 1 : 2 CTC TMPD-$TCNQ_2$ (projection 100). Stacks are parallel to c axis (reproduced with permission of Ref. 15).

the highly conducting ones for which a general model, taking into account both electron-electron and electron-phonon interactions, has been developed.[10] At the present stage a detailed comparison between experimental and theoretical results is still impossible owing to the complexity of the theories. These difficulties arise mainly from the electronic instabilities inherent to interacting one-dimensional Fermi systems (for a more detailed discussion see Ref. 7, Section IV.E).

TABLE 1

Schematic packing of the linear stacks in charge transfer complexes (CTC) and radical-ion salts (RIS)

Systems	Type of packing	Schematic packing	Examples
1 : 1 RIS	Regular	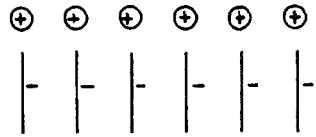	Rb-TCNQ (II)
1 : 1 RIS	Alternated	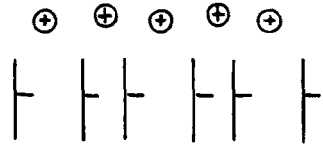	Rb-TCNQ (I)
n : m RIS	Regular	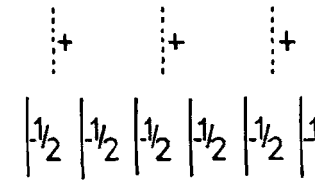	$Q\text{-}TCNQ_2$
n : m RIS	Alternated	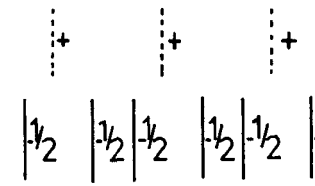	$TPP\text{-}TCNQ_2$
1 : 1 CTC	DA chain	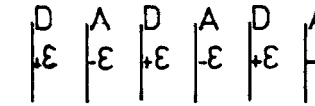	TCNQ-TMPD or TCNE-Pyrene (Figure 3)
1 : 1 CTC	Segregated RI chains	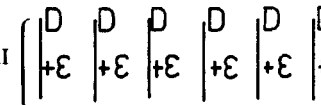	TTF-TCNQ
n : m CTC	Segregated RI chains	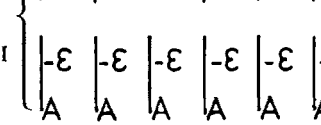	$TMPD\text{-}TCNQ_2$ (Figure 4)

† Abbreviations are given in the appendix.

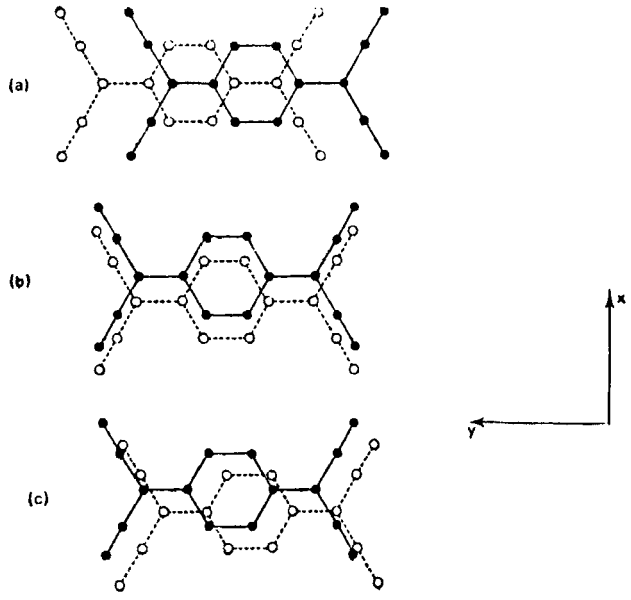

FIGURE 5 Typical overlaps for consecutive molecules in TCNO stacks[7]
a) Ring-external bond overlap $d(AB) = 3.25$ Å
b) Ring-ring overlap $d(BB') = 3.24$ Å
c) Unusual overlap $d(BB'') = 3.43$ Å.

A number of simplified models which are believed to be adapted to some particular systems and classes of properties, has been proposed (Ref. 5, Section 2). They involved either localized or itinerant electrons. As far as magnetic properties are concerned they range from a linear Heisenberg Hamiltonian,[17,19] with possible alternation, to a simple band model[20] with complete neglect of electron-electron interaction through a series of extended Hubbard type models.[21,22,29,55] Although the application of the Hubbard model to extended molecules is not entirely justified and although the "charge transfer integral" t and electron repulsion U become phenomenological parameters, it may help to understand the various features of the magnetic properties.[8] For small t/U ratios, the one-dimensional Hubbard Hamiltonian has been shown to reduce to the one-dimensional Heisenberg Hamiltonian with $J = 2t^2/U$. Adapted to the case of alternated chains this hamiltonian can be written as follows:

$$\mathcal{H} = J \sum_n \{(1 + \delta)\mathbf{S}_{2n} \cdot \mathbf{S}_{2n+1} + (1 - \delta)\mathbf{S}_{2n} \cdot \mathbf{S}_{2n-1}\} \qquad (1)$$

It seems flexible enough to describe many features of the real systems with localized moments.

In the following, we would like to take a more experimental point of view. We would try to show the qualitative informations which can be collected by ESR, rather than to present numerical results (usually obtained by forcing the experimental data into a maybe questionable model Hamiltonian). These qualitative informations may help to reveal the basic physical features of the systems:

a) The spin susceptibility on single crystals: although the susceptibility may be obtained by other methods, ESR measurements (Figure 6) may be more convenient for two reasons; at first experiments may be performed on very small samples; secondly it is possible to evaluate the contribution of the different magnetic species or of the chemically or crystallographically inequivalent stacks.

b) The type of elementary magnetic excitations and especially the presence of spatial correlation between spins ("triplet Frenkel excitons" or uncorrelated spins).

c) The spin dynamics: the ESR line shape is related to the spin time dependent correlation function which is strongly sensitive to the dimensionality. Two limiting behaviors are the wave propagation and the spin diffusion.[5]

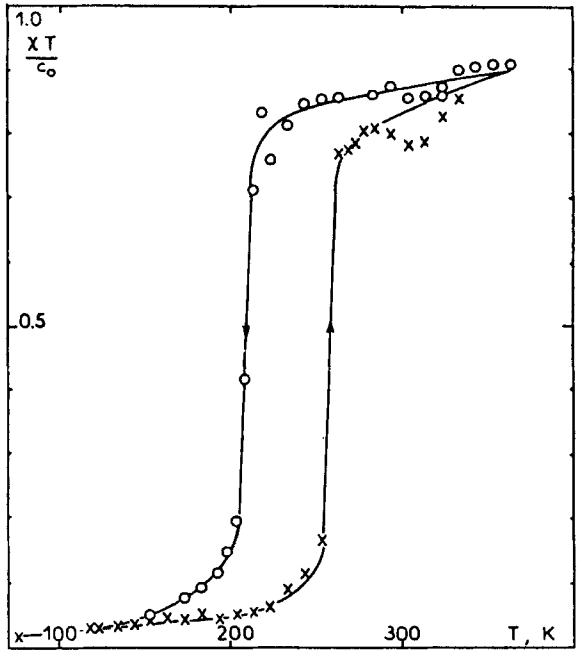

FIGURE 6 Temperature dependence of molecular magnetic susceptibility of CA^{-}-K^{+} obtained by ESR.[18]

d) Informations about the spin distribution obtained from the g values and eventually structural informations obtained from the comparison of the crystal g tensor to the molecular g tensor.

e) The order of magnitude of the coupling between chains which can perturb the one-dimensional behavior.

In order to illustrate these different points we present in a heuristic way some typical results chosen among either low conducting or highly conducting systems.

3 LOW CONDUCTING LINEAR SYSTEMS

Before discussing results concerning alternated and regular stacks of low conducting RIS and CTC, it is important to discuss the experimental difficulties to get properties *intrinsic to these systems.*

3.1 Impurity and intrinsic signals

An illustration of these difficulties is given by the susceptibility determination of Li^+–$TCNQ^-$ (Figure 7) for which two very different behaviors have been reported.[23,24] These differences may be due to a possible polymorphism (the crystalline structure has not yet been reported) or to the presence of impurities.

The correspondence between triplet signals and crystallophically alternated stacks and between a single line and regular stacks, as discussed in Sections 3.2 and 3.3, is an oversimplification which suffers many exceptions. Some alternated stacks never present a dipolar splitted signal, even at low excitation density where "exciton-exciton" interaction is believed to be small.[42] Moreover systems with triplet signals present generally a central "doublet" signal while regular stacks may present weak triplet satellites.[43] Attribution of these extra signals to "impurities" is questionable in systems where the excitation density remains very small. Although Curie behaviour has been found for the doublet signal of some systems as for example Rb^+–$TCNQ^-$ and K^+–$TCNQ^-$,[22] there are examples where the intensity of the doublet signal appears as an activated process.[44] Care has to be taken, from an experimental point of view, due to the possible presence of several components (broad and narrow) in the doublet and to the low powers requested to avoid saturation. Intrinsic effects, originating in the dissociation of the exciton as well as in the finite size of the chains have been invoked,[22] besides the paramagnetic impurities, without much conclusive evidence. This is a further reason to cast doubt on the analysis of the total

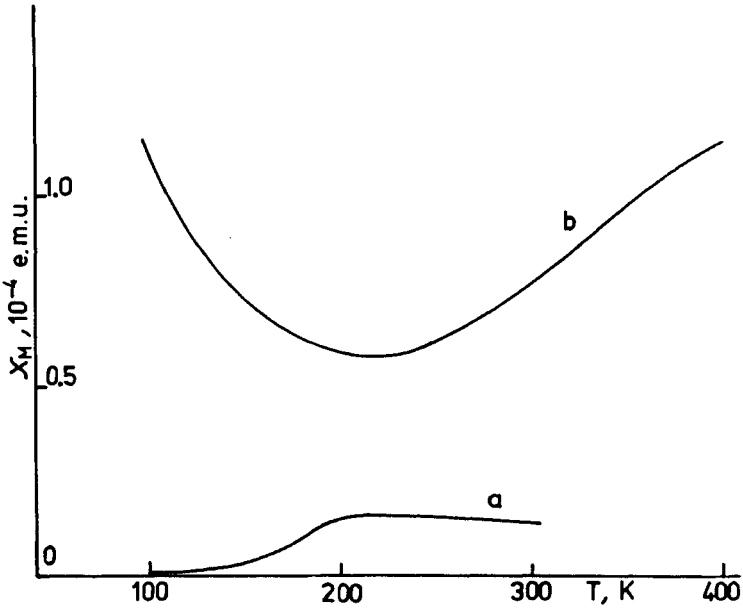

FIGURE 7 Temperature dependence of the molar spin susceptibility χ_M for Li-TCNQ: comparison between results of (a)[23] and (b).[24]

susceptibility with no reference to the corresponding ESR signals and to value susceptibility measurements by ESR over the standard methods, at low $\chi T/C$ values.

3.2 Alternated chains. The triplet exciton picture

We can picture a strongly alternated single chain as an assembly of weakly interacting "dimers" ($\delta \to 1$). The elementary excitations are therefore triplets which can jump along the chain, due to the small exchange integral $J(1 - \delta)$ between the adjacent RI belonging to two different pairs. In the isolated dimer approximation the susceptibility is given by:[8]

$$\chi = \frac{N}{1 + \frac{1}{3}\exp 2J/kT} \frac{g^2\beta^2}{3kT} \quad \text{and} \quad \rho = \chi T/C \tag{2}$$

where C is the Curie constant and ρ the thermal equilibrium concentration of triplet states. The values of J are generally small enough so that a large range of excitation density ρ can be explored at least when no structural phase transition modifies the alternation.

3.2.1 Low temperatures (small ρ) The existence of a triplet state resulting in a strong spatial correlation is ascertained by the presence of the characteristic fine structure resulting from the dipolar splitting (Figure 8). Since the Hamiltonian containing Zeeman and dipolar terms can be written as:

$$\mathcal{H} = g\beta\mathbf{H} \cdot \mathbf{S} + D(S_z^2 - S^2/3) + E(S_x^2 - S_y^2) \tag{3}$$

the two parameters D and E can be extracted from the angular dependence of the splitting (Figure 9) or from the powder spectra. These parameters can also be obtained from a quantum chemical calculation for a given geometry of the dimer.[62] In a crude approximation when spin densities are located on the atoms[27] and using the spin densities ρ_μ^s either obtained from the hyperfine structure of the ESR spectrum of the isolated RI in solution or resulting

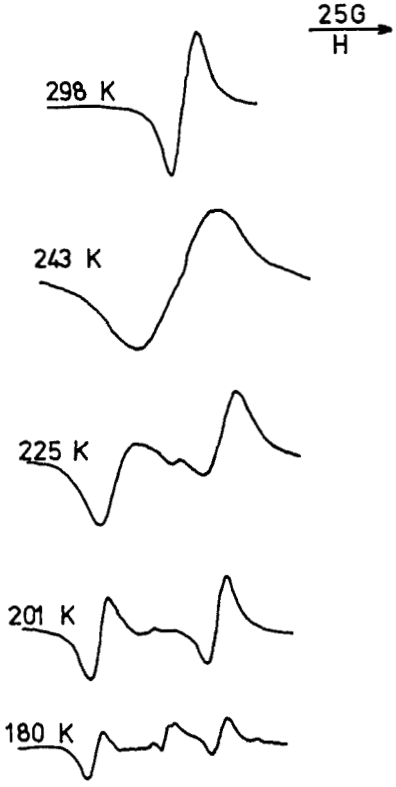

FIGURE 8 ESR spectra of a $(TMPD^+)_2$-$(Ni(mnt)_2)^{2-}$ crystal for an arbitrary orientation at several temperatures (taken from Ref. 25).

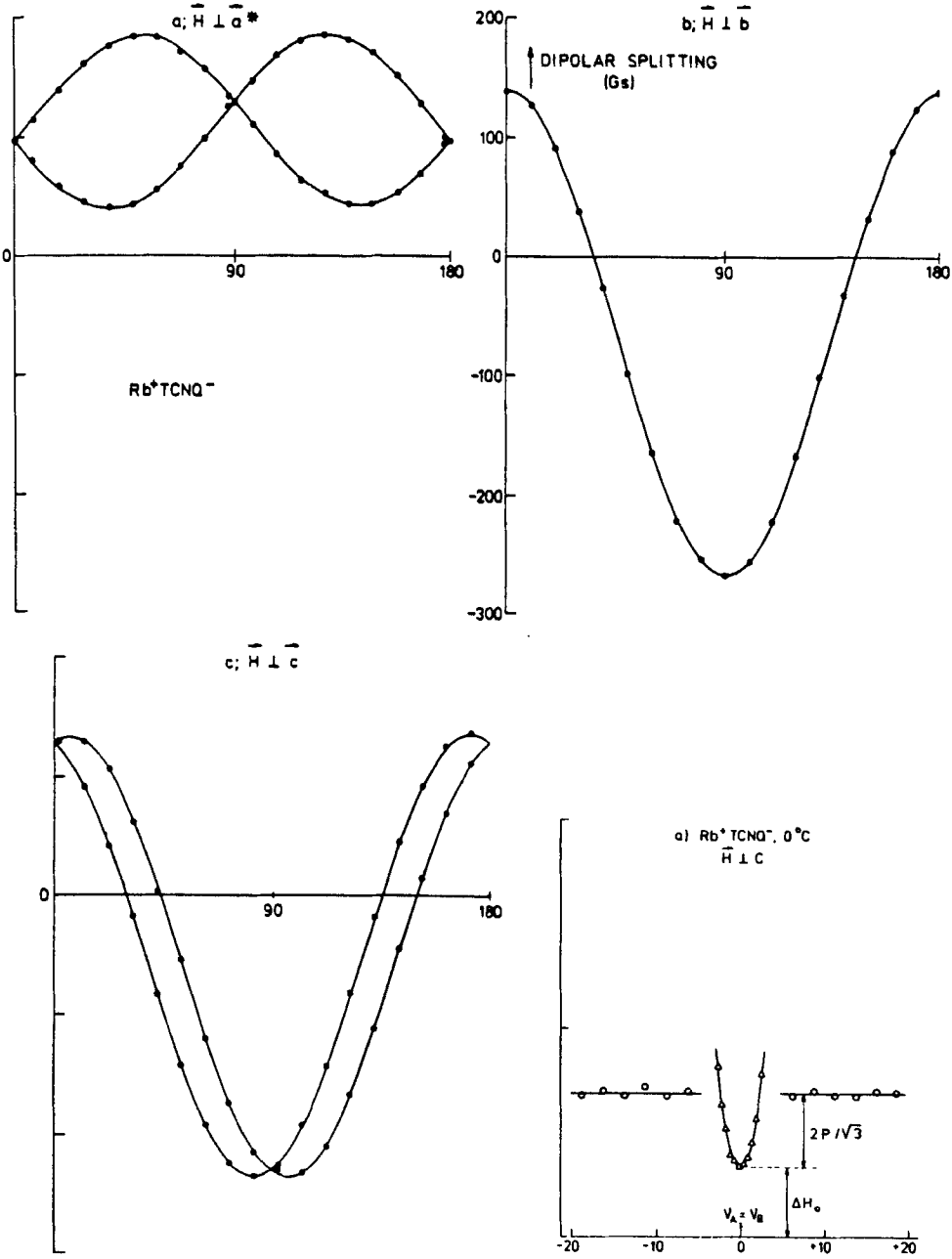

FIGURE 9 Dipolar splitting of Rb^+-$TCNQ^-$ for different crystal orientations and line width for one particular orientation (see text) (taken from Ref. 22).

from a quantum chemical calculation.

$$D = \tfrac{3}{4}g^2\beta^2 \sum_{\mu}\sum_{\nu} \rho^s_\mu \rho^s_\nu (r^2_{\mu\nu} - 3z^2_{\mu\nu}) r^{-5}_{\mu\nu} \tag{5}$$

$$E = \tfrac{3}{4}g^2\beta^2 \sum_{\mu}\sum_{\nu} \rho^s_\mu \rho^s_\nu (y^2_{\mu\nu} - x^2_{\mu\nu}) r^{-5}_{\mu\nu} \tag{6}$$

Typical results for alternated stacks with different stoichiometries are given in Table II. For some systems measured and calculated values are in disagreement. Assuming the dimer to consist of the "closest" molecules in the crystalline structure, this disagreement has been taken as a proof of a less complete spatial correlation.[22] However this interpretation has recently been questioned.[28]

TABLE II

Experimental and calculated zero-field splitting (ZFS) parameters in MHz.

Stoichiometry	System	Experimental		Calculated		Ref.
		$\|D\|$	$\|E\|$	$\|D\|$	$\|E\|$	
1 : 1	TMPD-C10$_4$	~0	212	13	236	56,57
	TMPD$_2$-Ni(mnt)$_2$	602	79.2	670	70	25
	M-TCNQ	450	53.8	464	44	57
	Rb-TCNQ(I)	400	49	617	69.7	58
2 : 3	Cs_2-TCNQ$_3$	281	45.3	262	34	59,58
1 : 2	ϕ_3PCH$_3$-TCNQ$_2$ / ϕ_3AsCH$_3$-TCNQ$_2$	186	29.4	186	22.5	60,58

Previously no mention has been made of the possible hyperfine structure (hf) resulting from electron-nuclear interaction and indeed none has been directly resolved. This is due to the fact that the small $J(1 - \delta)$ coupling (see Eq. 1) produces a fast enough motion of the triplet (Frenkel triplet exciton) to average out the major part of the hf interaction. Such a motion *along a stack* does not average out the dipolar interaction. A remaining influence of the hf interaction can however be detected from the anisotropy of the line width and from experiments with deuterated compounds ($\Delta\nu_{hf}$).[30] One would like to derive, from the importance of the averaging, an estimate of the triplet jump frequency. For a simple one-dimensional model Thomas and McConnell[27] have obtained the relation $\Delta\nu = (\Delta\nu^4_{hf}/\nu_{jump})^{1/3}$. Values of the jump frequency along the stack have been calculated but care must be taken of the fact that transverse jumps *between chains* are more efficient to average the hf splitting.[8]

The observation of the line width is complicated when there are several inequivalent chains in the crystal structure, like in K^+–$TCNQ^-$ and Rb^+–

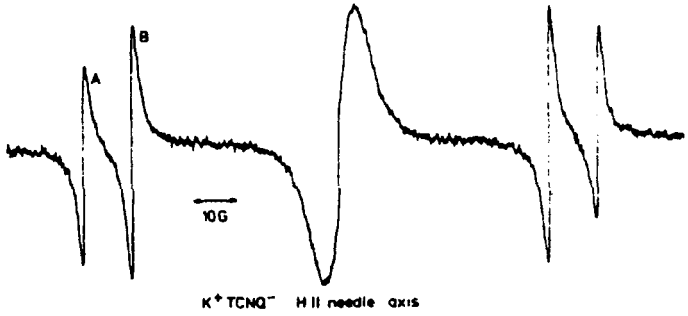

FIGURE 10 ESR spectrum of K^+-$TCNQ^-$ showing two magnetically inequivalent chains (taken from Ref. 22).

$TCNQ^-$.[22] They are revealed by a double triplet signal (Figure 10). Interchain jumps at a frequency ν_t are expected to broaden the line according to both following expressions:

$$\Delta\nu = \Delta\nu_0 + \nu_t \quad \text{in the slow jumping limit}$$

$$\Delta\nu = \tfrac{1}{2}(\Delta\nu_{0A} + \Delta\nu_{0B}) + (\nu_A - \nu_B)^2/\nu_t \quad \text{in the fast jumping limit.}$$

It is possible to change $\nu_A - \nu_B$ by a choice of the orientation and to measure both $\Delta\nu_0$ at $\nu_A = \nu_B$ and $\Delta\nu$ in the slow exchange regime for $\nu_A - \nu_B \gg \nu_t$ (Figure 9). Numerical values of ν_t and of its activation energy have been obtained in this way. ν_{jump} can in principle be calculated from $\Delta\nu_0$.

3.2.2 High Temperatures (large ρ) The jump frequency can also be derived from the changes, arising from exciton-exciton interaction, in line width and dipolar splitting as a function of ρ (Figure 8). The frequency of collision is given by:

$$\nu_e = \rho\nu_e^0 \sim \rho J(1 - \delta)/h$$

The line shape has been calculated by Lynden–Bell[32] and in a more complete way by Hibma.[22] This leads in the slow exchange limit to

$$\Delta\nu - \Delta\nu_0 = 2/(3\sqrt{3})A\rho\nu_e^0$$

$$d_0^2 - d^2 = 2(A\rho\nu_e^0)^2$$

where d is half the dipolar splitting, $\Delta\nu = \nu - g\beta_0 H/h$ and A measures the efficiency of the collision. It is difficult to evaluate A. The experiments show that it is an activated quantity. The activation energy is large and implies a diffusional process coupled to the vibrational distortions of the lattice.[22]

The dipolar splitting leads to a non arrhenian plot and to different values of d_0 according to the orientation. The line width variation seems more reliable.

3.3 Regular chains

In all crystallographically regular chains, either of the RI type or of the CTC type with segregated or mixed chains, the ESR signal appears as a single line.

In many cases, once the contribution of impurities at low temperatures has been subtracted, susceptibilities can be fitted to an activated process $\chi T\alpha \exp - \Delta E/kT$. ΔE is generally rather large, except in very few cases, so that one is restricted—due to the material instability at temperatures above 350–400 K—to a narrow range of excitation densities ρ; the behaviour is therefore very unspecific. No theoretical model is able, at the present stage, to give a reasonable account for the origin of ΔE (contrary to the alternated model discussed in Section 3.2). Information is therefore mostly derived from the variation of line width, line shape and line position with temperature, rationalized in terms of variation with the excitation density ρ. Measurements at at least two resonance frequencies are generally requested to unambiguously distinguish between field dependent and field independent contributions.

The crystal g factor and its anisotropy may yield informations about structure and spin distribution. It is possible to determine a molecular g factor from a RI compound whose crystalline structure is known. For systems whose crystalline structure is not known, the orientation of the RI with respect to the crystal axes can then be derived from the angular dependence of the g factor (Figure 11). In the case of RI with organic counter-ions this procedure assumes that all the spins are distributed on the RI chains. Such an assumption is often supported by comparing the mean g factor of the crystal to that obtained in solution; however it can be questioned from the NMR second moment measurements as recently shown in NMP–TCNQ where dipolar interaction between electrons and NMP protons seems to be non negligible.[34]

For some CTC it has been possible to estimate on which stack, the spins are distributed by comparing the crystal mean g value to the mean value for the radical-ions derived from the donor and acceptor in solution.

The line width and its angular and thermal dependence is of more interest. It has been shown that an *assumption of uniform magnetic dilution*, at least at small ρ values with a complete absence of spatial correlation between spins, is in agreement with several characteristics of the signal.[8] The elementary excitations involved in such a description have been called "Wannier excitons" in contrast to the case of strongly correlated spins, or "Frenkel

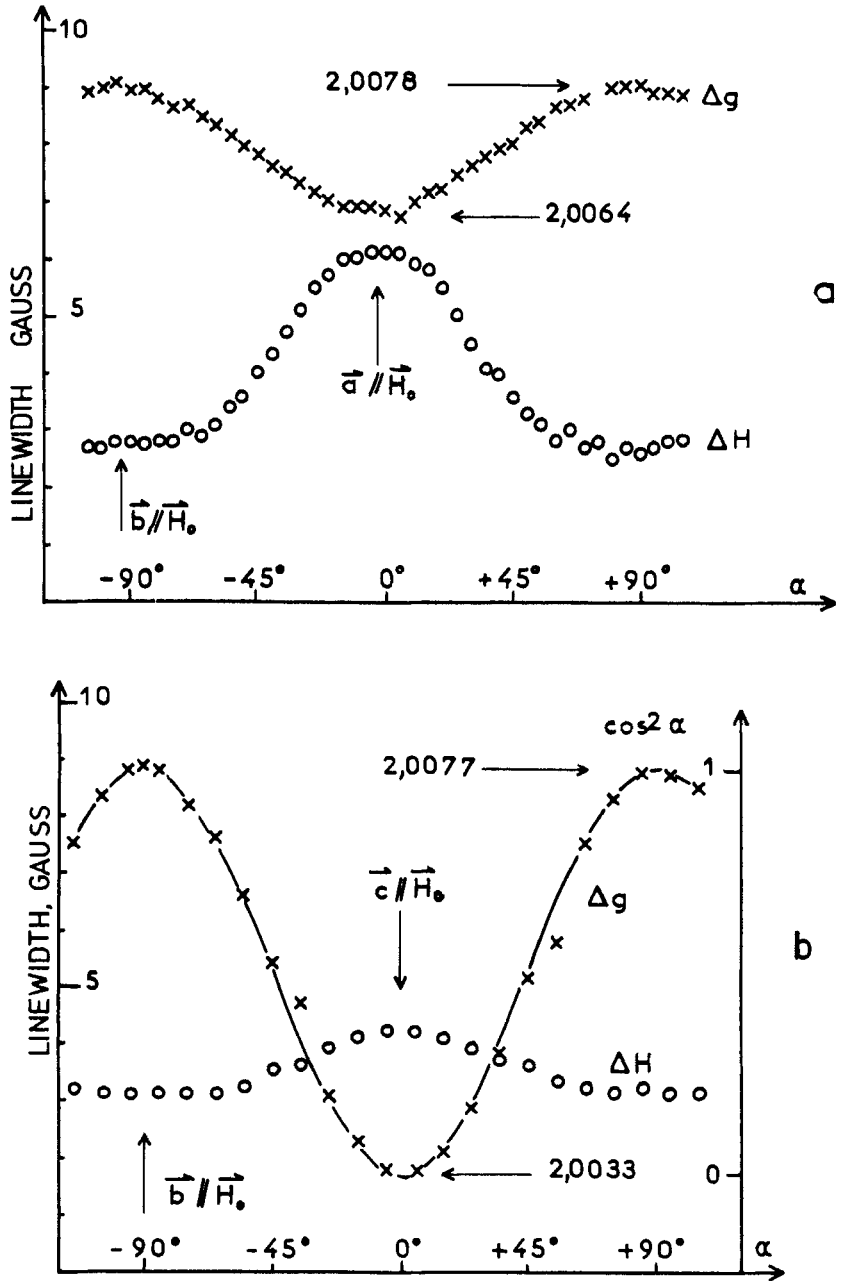

FIGURE 11 g-factor (x) and line-width (0) tensors of CA^{-}–K^{+}. g-factor deflections from the free electron $g = 2.0023$ are given in gauss (taken from Ref. 18).

excitons," in the alternated chains. The indications in favour of this assumption are:

1) the absence of fine splitting

2) the angular dependence of the line width which has the shape expected for the electronic second moment, as calculated from the spin densities on the radical-ions scaled according to a proportionality factor equal to ρ (Figure 12).

3) the variation of line shape with ρ.

Under this assumption of magnetic uniform dilution the electron-electron dipolar interaction should scale as ρ to give a second moment ρM_2^0.[8] However exchange interaction will reduce this dipolar interaction, and the exchange frequency should also scale according to $\rho : \nu_e = \rho \nu_e^0$. Taking

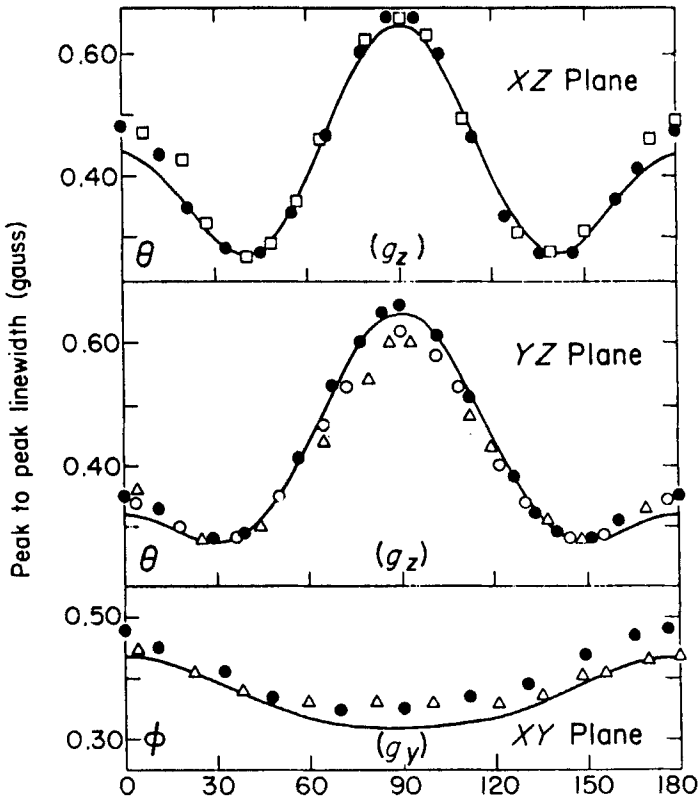

FIGURE 12 Angular dependence at 300 K of the ESR linewidth of TMPD–CA in the three principal axis planes of the g-tensor.[35]

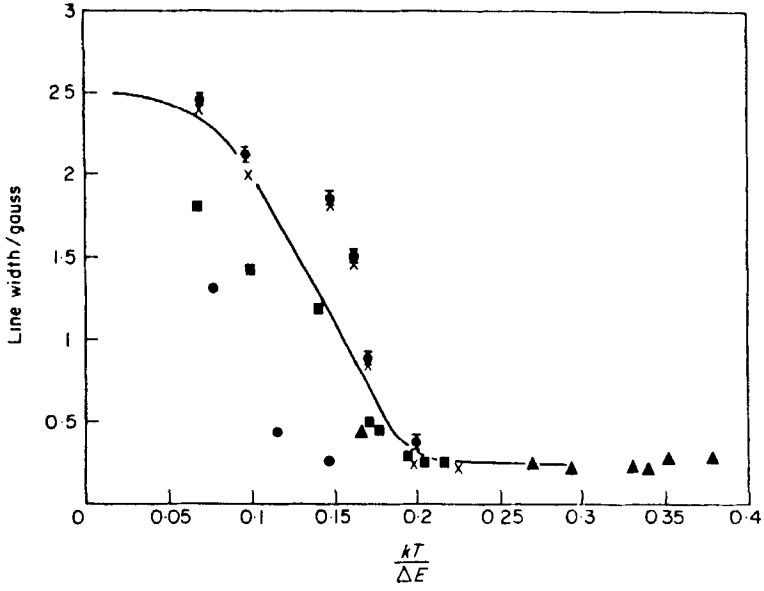

FIGURE 13 Peak-to-peak ESR linewidth for three DA chains CTC at Q band as a function of $kT/\Delta E_p$. The ■, × and ◆ refer to three different PD-CA samples ($\Delta E = 0.13$ eV): ▲ refers to TMPD-TCNQ ($\Delta E = 0.07$ eV): ● refers to TMPD-CA ($\Delta E = 0.15$ eV) (taken from Ref. 37).

into account the residual line width arising from hf coupling, relaxation effects, impurities, one expects in a rough approximation:

$$\Delta\nu\alpha(\rho M_2^0 + \text{constant})/\rho\nu_e^0$$

Indeed variation of line width for several CTC regular stacks seems to fit a ρ dependence (Figure 13) in agreement with the above formula using a nearly independent line width at high enough ρ (in contrast with the line width of an exchange narrowed collapsed signal in the case of triplet Frenkel excitons). A value of ν_e can then be derived.

Another indication for the role of the scaled second moment in the control of the ESR line width has been deduced from its variation, observed at high ρ, in the compound TMPD–TCNQ where an exceptionnally small ΔE gives access to high ρ. The peculiar variation of line width (Figure 14) with ρ has been attributed to the 10/3 effect, i.e. the replacement of the truncated Van Vleck second moment by the full second moment when the actual exchange frequency $\rho\nu_e^0$ becomes of the order of the electronic Larmor frequency. This interpretation is substantiated by the T_1 behaviour as a function of temperature (however T_1 has been deduced from progressive saturation by assuming a Lorentzian line shape).[36]

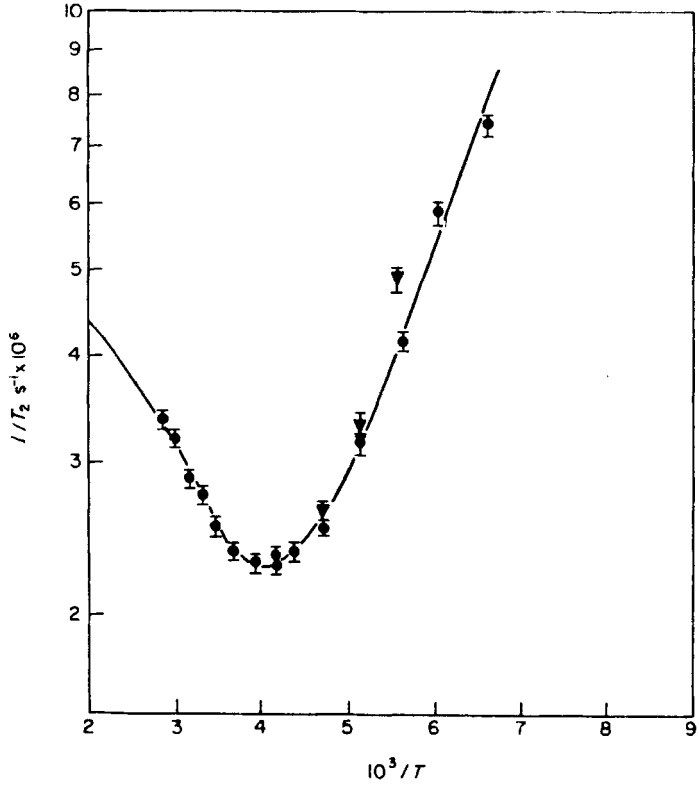

FIGURE 14 Temperature dependence of the ESR linewidth (T_2^{-1}) in TMPD-TCNQ at X band showing the "10/3" effect when $\rho\omega_c^0$ exceeds the Larmor frequency at high temperatures (taken from Ref. 36).

Nevertheless such an approximate treatment does not take into account the peculiarities of a nearly one-dimensional system. Direct evidence for a very weak interchain coupling can be derived from the existence, in the regular stacks of PD–CA, of three distinguishable signals arising from three crystallographically inequivalent chains.[37] Since the splittings (the nature of which is controlled by X and Q band measurements) is smaller than 1 gauss, the interchain coupling must be very small. It disappears at higher ρ, the dipolar interaction between inequivalent chains becoming high enough as compared to the splitting (Figure 15).

The general theories of magnetic resonance related the width of an exchange narrowed line to the amplitude of local dipolar and hf fields and, in the high temperature range where ρ is large, to Fourier components of the spin correlation function. For the one-dimensional case, the analysis by

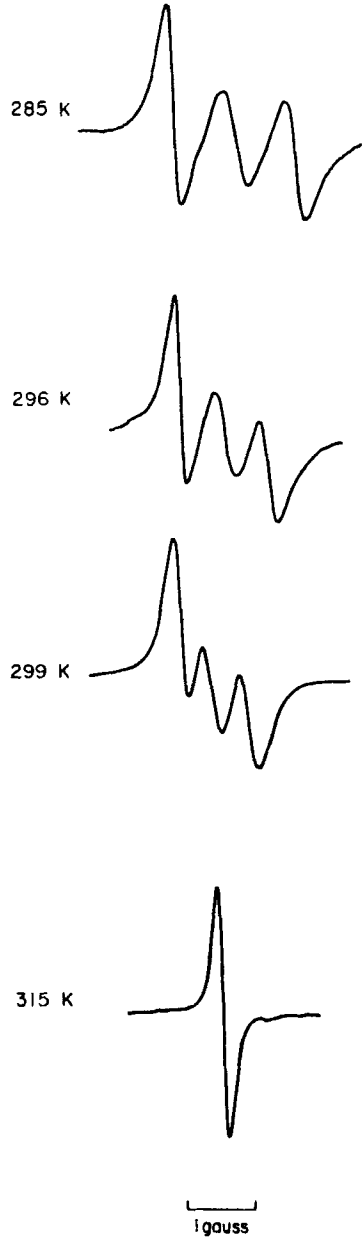

FIGURE 15 a) Temperature dependence of the ESR in PD-CA, showing the collapse of the g-factor splittings. The sweep, but not the gain, is the same for all four spectra.

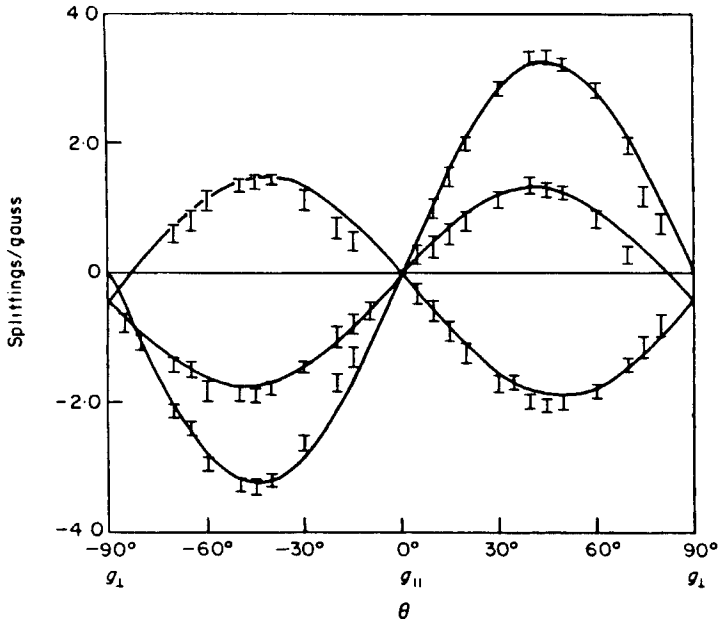

FIGURE 15 b) Comparison of the angular dependence of the Q-band g-factor splittings in PD-CA at 263 K arising from magnetically inequivalent stacks with theory for three identical noninteracting stacks. (Taken from Ref. 37).

Hone and Richards[1] predicts a line width varying like $\rho^{1/3}$ and a non lorentzian (and non gaussian) behaviour (Figure 16). This is due to the peculiar $t^{-1/2}$ dependence of the spin autocorrelation function. This long time memory and the corresponding divergence of the power spectrum at $\nu \to 0$ is characteristic of one-dimensional systems. However it is easy to realize that any slow process like transverse interaction will play an important role in the long time behaviour of the spin autocorrelation function and therefore play an important role on the low frequency part of the power spectrum responsible of the line shape. This can lead to a more "classical" line shape and to a modified expression of the line width as proposed by Huang and Soos.[38]

$$\Delta\nu\alpha(\rho M_2^0 + \text{constant})/(2\nu_e\nu_t)^{1/2}$$

where ν_t is the transverse exchange frequency; its ρ dependence is still a matter of discussion.

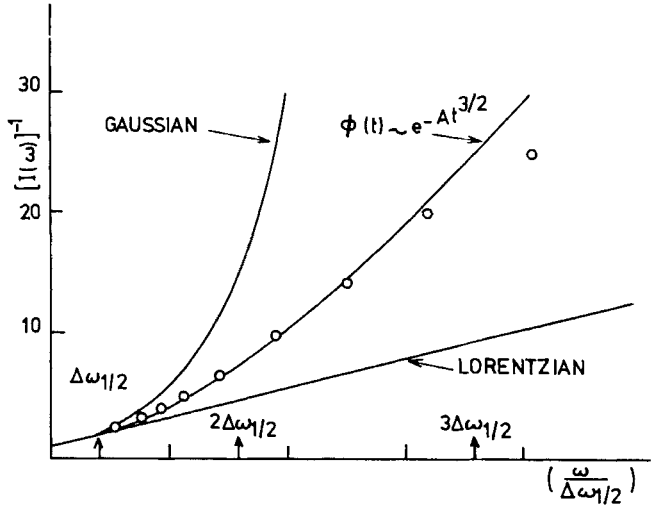

FIGURE 16 Comparison between theory and experiment for the ESR lineshape in the one-dimensional system TMMC. The theoretical calculations fit to the experiment (open circles) (taken from Ref. 54).

Up to now ESR line shape analysis appears to be much more difficult to interpret than the NMR relaxation. Due to the low nuclear Larmor frequency, this latter is much more sensitive to the details of the spin autocorrelation function to which the nuclei are coupled through the scalar and dipolar parts of the hf coupling. Indeed a low frequency $\nu^{-1/2}$ dependence of the proton T_1 has been found in several CTC and RI systems at low frequency with a *crossover* to a frequency independent regime.[39,40] The crossover value of the frequency gives an estimate of the correlation time associated with interchain hopping. For the particular case of a cubic lattice with arbitrary anisotropy, the crossover regimes have been discussed recently.[41] Line shapes and line widths of ESR spectra can then be used for a check of consistency.

4 HIGHLY CONDUCTING LINEAR SYSTEMS

Susceptibility measurements performed on a number of highly conducting salts are schematically reported on Figure 17. For comparison the susceptibility of a non conducting system is also shown. A nearly temperature independent molar susceptibility 0.3 to 0.6 10^{-3} emu is observed at high tem-

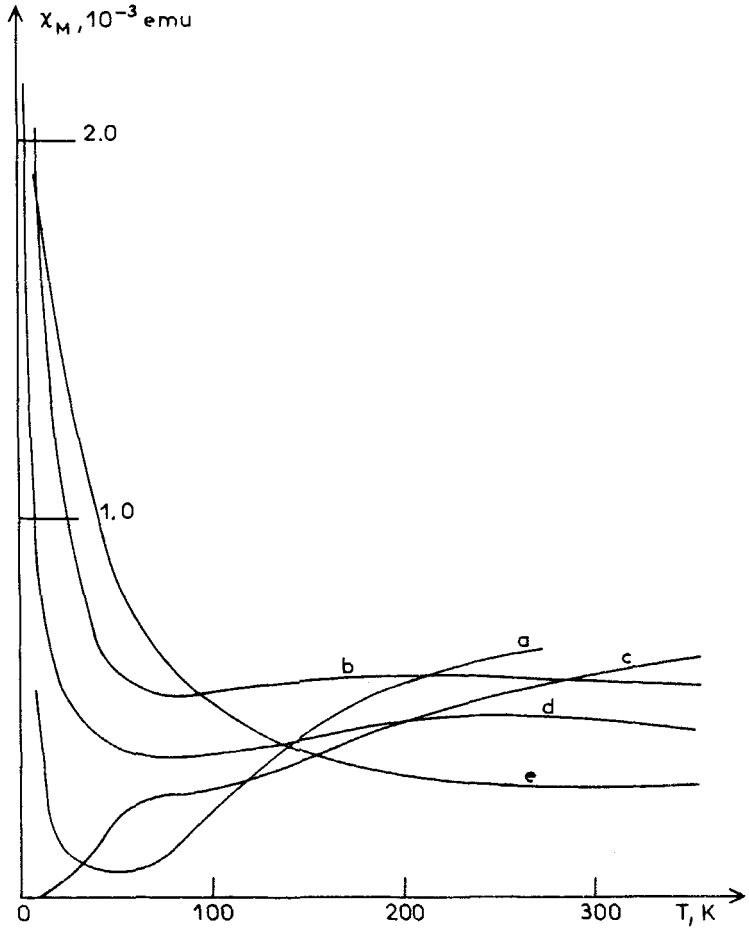

FIGURE 17 Temperature dependence of the molar magnetic susceptibility of some TCNQ compounds: a) TEA-$TCNQ_2$,[45] b) Ac-$TCNQ_2$,[46] c) TTF-TCNQ,[47] d) Q-$TCNQ_2$,[46] e) NMP-TCNQ.[46,48] (Taken from Ref. 7).

peratures. The case of CTC with segregated RI chains is complicated by the fact that each type of stacks may contribute differently to physical properties. The details of the susceptibilities at lower temperatures are however very different according to the type of compound and reflect in some cases the existence of anomalies in the conductivity behaviour.[47,48] The very low temperature behaviour has recently raised much interest since a power law behaviour $T^{-\alpha}$ seems to have been detected in several RI salts.[49,50]

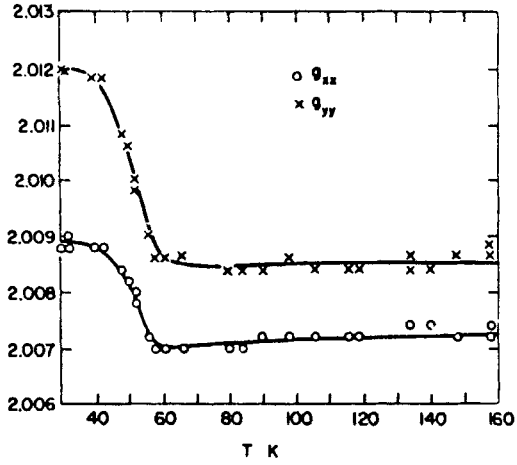

FIGURE 18 The principal g values g_{xx} and g_{yy} as a function of temperature of TTF-TCNQ (taken from Ref. 51).

Line shapes analysis is complicated by the Dysonian line shape resulting from spin diffusion in the skin depth, at least for the orientation corresponding to the largest conductivity. ESR can however be of some help in the case of segregated CTC, where both stacks are potentially one-dimensional conductors at high temperature, to understand interchain coupling, especially near the low temperature transitions.

The more detailed measurements have been carried out by Tomkiewicz *et al.*[51,52,53] in TTF-TCNQ crystals, taking advantage of the large g factor difference between TTF^{+} ($\bar{g}$ = 2,00838) and $TCNQ^{-}$ ($\bar{g}$ = 2,00268) radical-ions, together with relaxation measurements from progressive saturation experiments.

In the metallic state ($T > 60$ K) the constant intermediate g factor (Figure 18) and the decrease in the width of the Lorentzian signal, which is field independent, cannot both be fully explained either by a strong or a weak interchain coupling assumption. A weak coupling with a larger contribution of TTF stack to the conductivity and a larger contribution of TCNQ stack to the susceptibility has however been proposed.[52]

In the low temperature range, a gradual shift of g towards the TTF value, the variation of line width with temperature Figure 19 and the line width anisotropy are in favour of a strong coupling between chains. However this coupling allows a separation of the TTF and TCNQ contributions to the overall susceptibility (Figure 20). χ_{TCNQ} decreases strongly below 54 K while χ_{TTF} decreases only below 38 K, these two temperatures corresponding to two of the three known transitions detected by X-ray scattering.[16]

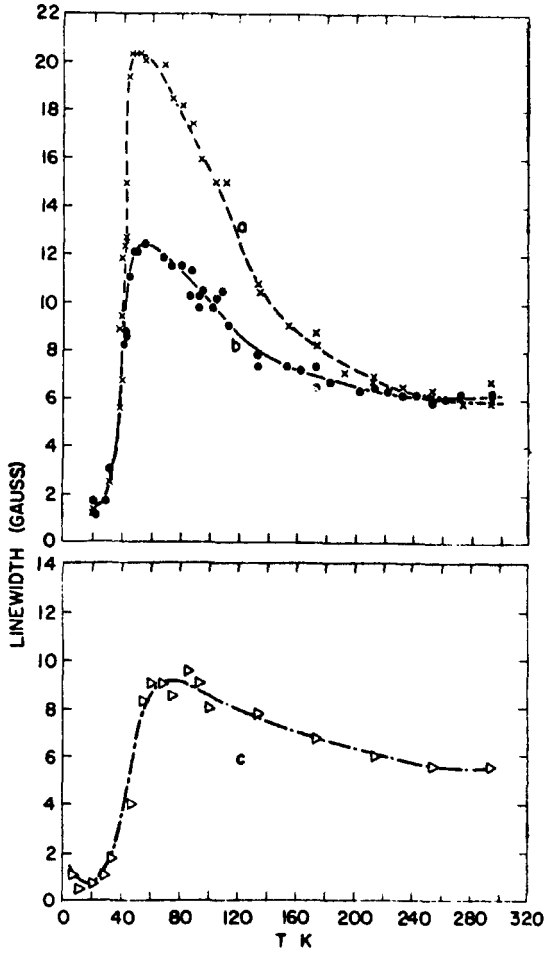

FIGURE 19 Variation of ESR linewidth with temperature with the magnetic field parallel to the principal axes for TTF-TCNQ. Curves *a* and *b* are for $\mathbf{H}_1 \parallel \mathbf{b}$ while curve *c* is for $\mathbf{H}_1 \perp \mathbf{b}$ (taken from Ref. 51).

In the isostructural compound $(TSeF)_x(TTF)_{1-x}$-TCNQ in the metallic state a dramatical line width variation ($5 \rightarrow 500$ *G*) as a function of x has been observed by the same authors (Figure 21). Due to the very large value g (2,027) of the selenated compound an interpretation based on a relaxation mechanism involving a combination of spin–orbit and electron–phonon interaction has been proposed. It predicts a Δg^2 proportionality for the linewidth.[53]

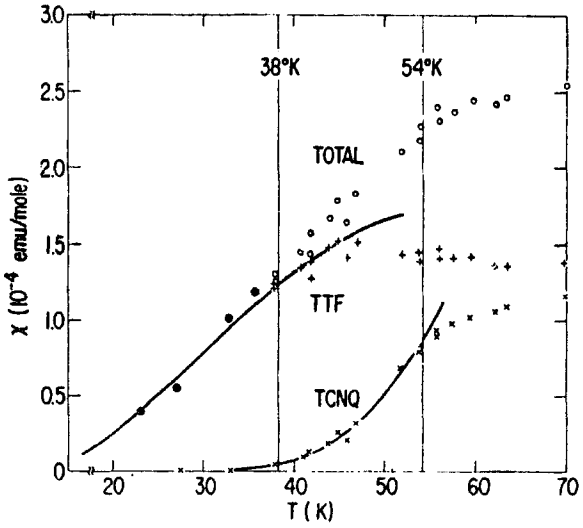

FIGURE 20 The susceptibilities of the individual chains and the total measured susceptibility of TTF-TCNQ. The full lines corresponding to the calculated values obtained from activation energies $\Delta_{TTF} = 94$ K and $\Delta_{TCNQ} = 400$ K (taken from Ref. 52).

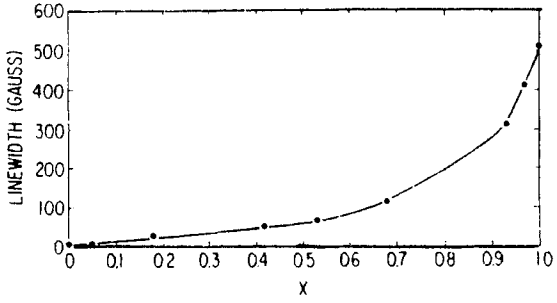

FIGURE 21 Linewidth dependence for $\mathbf{H}_{dc} \parallel c'$ direction on x. The measurements were taken at 300 K on a single crystal $TTF_{(1-x)}$. $TSeF_x$-TCNQ (taken from Ref. 53).

5 CONCLUSION

From all these results concerning low and highly conducting systems it has been possible to get invaluable information: existence of magnetically inequivalent sites, respective contributions of the different magnetic species; in particular cases, the existence of weak intrachain coupling has been pointed out and even some order of magnitude for the ratio of intra- to interchain exchange have been reached. However it is obvious that the informations

derived from ESR measurements must always be critically considered, the attribution of the effects observed to a leading mechanism requiring generally many complementary measurements (such as deuteration for example). This is particularly true for the understanding of the dynamic properties which need different techniques like NMR, inelastic neutron scattering.[1] NMR is more sensitive to the dimensionality of the spins systems than ESR for which no dimensionality effect has been observed (line shape) on these organic systems.[39] The most powerful technique, the neutron scattering, has allowed on the highly conducting system TTF–TCNQ, to get a very detailed picture of the dynamics of the itinerant electrons.[61]

Note added in proof

In connection with dimensionality effects, half field ESR transitions resulting from the tail of the spin autocorrelation function in 1 and 2 dimensional magnets have been recently discussed and found in inorganic systems TMMC and K_2MnF_4.[63,64]

Appendix: Abbreviations

Triethylammonium	TEA
Triphenylmethylphosphonium	ϕ_3PMe
Tetraphenylphosphonium	TPP
Triphenylmethylarsonium	ϕ_3AsMe
Morpholinium	M
Quinolinium	Q
Acridinium	Ac
N-methylphenazinium	NMP
p-phenylenediamine	PD
N,*N*,*N*′,*N*′tetramethyl-*p*-phenylenediamine	TMPD
2,2′-Bis-1,3 dithiole or tetrathiofulvalene	TTF
tetraselenofulvalene	TSeF
Nickel-bis-cis 1,2 dicyano ethylene-1,2 dithiolate	$Ni(mnt)_2$
Tetracyanoethylene	TCNE
7,7,8,8,Tetracyanoquinodimethane	TCNQ
2,3,5,6 tetrachloro-*p*-benzoquinone or *p*-chloranil	CA
Tetramethyl-ammonium chloride	TMMC

References

1. D. W. Hone and P. M. Richards, *Ann. Rev. Mat. Sci.*, **4**, 337 (1974).
2. P. M. Richards, in Proceedings of the International School of Physics Enrico Fermi. Course LIX: Local Properties at Phase Transitions, 1973 (North-Holland, Amsterdam, 1976), pp. 539–606.
3. L. J. de Jongh and A. R. Miedema, *Adv. Phys.*, **23**, 1 (1974).
4. J. S. Miller and A. J. Hepstein, *Prog. Inorg. Chem.*, **20**, 1 (1975).
5. M. Steiner, J. Villain and C. G. Windsor, *Adv. Phys.*, **25**, 87 (1976).
6. See also the following proceedings of meetings; *One Dimensional Conductors*, ed. J. Ehlers, K. Hepp and H. A. Weidmuller, GPS Summer School Proceedings, Lecture Notes in Physics (Springer-Verlag, Berlin, 1975); *Low Dimensional Cooperative Phenomena: The Possibility of High Temperature Superconductivity*, ed. H. J. Keller, NATO ASI, Series B, Volume 7, 1975; Proceedings of the IVth International Symposium on the Organic Solid State, Bordeaux, 1975, *Mol. Cryst. Liq. Cryst.*, **32**, pp. 1–270 (1976).
7. J. J. Andre, A. Bieber and F. Gautier, *Ann. de Phys.*, 15 ème série, **1**, 145 (1976).
8. Z. G. Soos and D. J. Klein, in *Molecular Association*, ed. R. Foster, (Academic Press, New York, 1975), vol. 1, pp. 1–109.
9. P. L. Nordio, Z. G. Soos and H. M. McConnell, *Ann. Rev. Phys. Chem.*, **17**, 237 (1966).
10. L. Mihaly and J. Solyom, *J. Low Temp. Phys.*, **24**, 579 (1976).
11. B. L. Bales, *Chem. Phys. Lett.*, **10**, 361 (1971).
12. J. H. Van Vleck, *Phys. Rev.*, **74**, 1168 (1948).
13. P. W. Anderson and P. R. Weiss, *Rev. Mod. Phys.* **25**, 269 (1953).
14. I. Ikemoto and H. Kuroda, *Acta Cryst.*, **B24**, 383 (1968).
15. A. W. Hanson, *Acta Cryst.*, **B24**, 768 (1968).
16. P. Bak and V. J. Emery, *Phys. Rev. Lett.*, **36**, 978 (1976).
17. P. M. Richards and F. Carboni, *Phys. Rev.*, **B5**, 2014 (1972).
18. J. J. Andre and G. Weill, in *Quelques Aspects de l'Etat Solide Organique*, ed. J. P. Suchet (Masson et Cie, Paris, 1972), vol. 5, pp. 127–139.
19. Z. G. Soos, *J. Chem. Phys.*, **43**, 1121 (1965).
20. P. A. Fedders and J. Kommandeur, *J. Chem. Phys.*, **52**, 2014 (1970).
21. a) P. J. Strebel and Z. G. Soos, *J. Chem. Phys.*, **53**, 4077 (1970); b) Z. G. Soos and P. J. Strebel, *J. Am. Chem. Soc.*, **93**, 3325 (1971); c) Z. G. Soos and P. J. Strebel, *J. Chem. Phys.*, **55**, 3284 (1971).
22. T. Hibma, Ph. D. Thesis, University of Groningen, 1974.
23. S. K. Khanna, E. Ehrenfreund, E. F. Rybaczewski, and S. Etemad, Proceed. of Conference on Magnetism and Magnetic Materials, Denver, 1972, p. 1509.
24. J. G. Vegter, P. I. Kuindersma, and J. Kommandeur, Proceedings of the Conference on Conduction in Low Mobility Materials, Eilat (Israel), 1971, p. 363.
25. M. J. Hove, B. M. Hoffman, and J. A. Ibers, *J. Chem. Phys.*, **56**, 3490 (1972).
26. T. Hibma and J. Kommandeur, *Phys. Rev.*, **B12**, 2608 (1975).
27. D. D. Thomas, H. Keller, and H. M. McConnell, *J. Chem. Phys.*, **39**, 2321 (1963).
28. A. J. Silberstein and Z. G. Soos, *Chem. Phys. Lett.*, **39**, 525 (1976).
29. F. Devreux, *Phys. Rev.*, **B13**, 4651 (1976).
30. T. D. Buckman, O. H. Griffith, and H. M. McConnell, *J. Chem. Phys.*, **43**, 2907 (1965).
31. M. Konno, H. Kobayashi, F. Marumo, and Y. Saito, *Bull. Chem. Soc. Japan*, **46**, 1987 (1973).
32. R. M. Lynden-Bell, *Mol. Phys.*, **8**, 71 (1964).
33. M. T. Jones and D. B. Chesnut, *J. Chem. Phys.*, **38**, 1311 (1963).
34. M. A. Butler, F. Wudl, and Z. G. Soos, *Phys. Rev.*, **B12**, 4708 (1975).
35. T. Z. Huang, R. P. Taylor, and Z. G. Soos, *Phys. Rev. Lett.*, **28**, 1054 (1972).
36. B. M. Hoffman and R. C. Hughes, *J. Chem. Phys.*, **52**, 4011 (1970).
37. R. C. Hughes and Z. G. Soos, *J. Chem. Phys.*, **48**, 1066 (1968).
38. T. Z. Huang and Z. G. Soos, *Phys. Rev.*, **B9**, 4981 (1974).
39. F. Devreux and M. Nechtschein, *Sol. St. Comm.*, **16**, 275 (1975).

40. D. Jerome, Proceedings of NATO ASI on Chemistry and Physics of one-dimensional Metals, Bolzano, 1976.
41. M. A. Butler, L. R. Walker, and Z. G. Soos, *J. Chem. Phys.*, **64**, 3592 (1976).
42. S. K. Khanna, A. A. Bright, A. F. Garito, and A. J. Heeger, *Phys. Rev.*, **B10**, 2139 (1974).
43. J. J. Andre, unpublished results: Triplet excitons have been found on polycrystalline samples of CA–K, CA–Li at room temperature. For CA–K which has a regular stacking[31] $D = 695$ MHz and $E = 64.5$ MHz and for CA–Li $D = 795$ MHz and $E = 68.8$ MHz. On CA–Na samples two species have been distinguished with $D = 695$ and 563 MHz and $E = 48$ and 6 MHz respectively. All these triplet excitons are present at a too low concentration to be observed on single crystals.
44. G. T. Pott, C. F. Van Bruggen, and J. Kommandeur, *J. Chem. Phys.*, **47**, 408 (1967).
45. R. G. Kepler, *J. Chem. Phys.*, **39**, 3528 (1963).
46. L. N. Bulaevskii, A. V. Zvarykina, Yu S. Karimov, R. B. Lyubovskii, and I. F. Shchegolev, *Soviet Phys. JETP*, **35**, 384 (1972) (*ZheTF*, **62**, 725 (1972)).
47. J. C. Scott, A. F. Garito, and A. J. Heeger, *Phys. Rev.*, **B10**, 3131 (1974).
48. A. J. Epstein, S. Etemad, A. F. Garito, and A. J. Heeger, *Phys. Rev.*, **B5**, 952 (1972).
49. I. F. Shchegolev, *Phys. Stat. Sol.*, **a12**, 9 (1972).
50. L. J. Azevedo and W. G. Clark, Proceedings of NATO ASI on Chemistry and Physics of one-dimensional Metals, Bolzano, 1976.
51. Y. Tomkiewicz, B. A. Scott, L. J. Tao, and R. S. Title, *Phys. Rev. Lett.*, **32**, 1363 (1974).
52. Y. Tomkiewicz, A. R. Taranko, and J. B. Torrance, *Phys. Rev. Lett.*, **36**, 751 (1976).
53. Y. Tomkiewicz, E. M. Engler, and T. D. Schultz, *Phys. Rev. Lett.*, **35**, 456 (1975) (see also Y. Tomkiewicz, A. R. Taranko, and E. M. Engler, *Phys. Rev. Lett.*, **37**, 1705 (1976)).
54. R. E. Dietz, F. R. Merritt, R. Dingle, D. Hone, B. G. Silbernagel, and P. M. Richards, *Phys. Rev. Lett.*, **26**, 1186 (1971).
55. G. Keryer and P. Delhaes, to be published.
56. D. D. Thomas, H. Keller, and H. M. McConnell, *J. Chem. Phys.*, **39**, 2321 (1963).
57. M. A. Marechal and H. M. McConnell, *J. Chem. Phys.*, **43**, 497 (1965).
58. T. Hibma, P. Dupuis, and J. Kommandeur, *Chem. Phys. Lett.*, **15**, 17 (1972).
59. D. B. Chesnut and P. Arthur, Jr., *J. Chem. Phys.*, **36**, 2969 (1962).
60. D. B. Chesnut and W. D. Phillips, *J. Chem. Phys.*, **35**, 1002 (1961).
61. R. Comes, G. Shirane, S. M. Shapiro, A. F. Garito, and A. J. Heeger, *Phys. Rev.*, **B14**, 2376 (1976); G. Shirane, S. M. Shapiro, R. Comes, A. F. Garito, and A. J. Heeger, *Phys. Rev.*, **B14**, 2325 (1976) and references therein.
62. Y. Gondo and A. H. Maki, *J. Chem. Phys.*, **50**, 3270 (1969).
63. K. Nagata, I. Yamada, T. Komatsubara, and T. Nishizaki, *J. Phys. Soc. Japan*, **43**, 707 (1977).
64. A. Lagendijk and D. Schoemaker, *Phys. Rev.* **B16**, 47 (1977).